scientific reports

Check for updates

OPEN

An innovative dual recognition aptasensor for specific detection of *Staphylococcus aureus* based on Au/Fe_3O_4 binary hybrid

Mohamed M. El-Wekil[1]✉, Hamada Mohamed Halby[2], Mahmoud Darweesh[2,3], Mohamed E. Ali[2] & Ramadan Ali[4]

Pathogenic bacteria cause disease outbreaks and threaten human health, prompting the research on advanced detection assays. Herein, we developed a selective molecular imprinted aptasensor for sensitive and prompt quantitation of *Staphylococcus aureus* (*S. aureus*) bacteria. The aptasensor was constructed by immobilization of aptamer on gold nanoparticles modified magnetic nanoparticles (apt-AuNPs@ Fe_3O_4). A functional monomer (o-phenylenediamine, o-phen) was electro-polymerized on the surface of the as-synthesized nanocomposite in the presence of a template (*S. aureus*). After removing *S. aureus*, the formed imprinted sites were available to extract pathogenic bacteria from complicated matrices. The surface morphology of the as-fabricated nanocomposites was characterized using different spectroscopic and electrochemical methods. Moreover, we thoroughly evaluated factors affecting the synthesis and determination procedures. The molecular imprinted aptasensor exhibited a wide linear range of 10^1–10^7 CFU mL^{-1} with a Limit of Detection, LOD (signal to noise = 3) of 1 CFU mL^{-1}. The aptasensor detected *S. aureus* in milk, conduit water, and apple juice samples with good recoveries % and satisfactory relative standard deviations (RSDs %) values.

A Gram-positive bacterium, staphylococcus aureus (S. aureus) is an extremely significant food-borne pathogenic bacteria. Its harmful effects on humans include pneumonia, endocarditis, abscesses, and septicemia[1]. It was reported that *S. aureus* is highly infectious and causes some of the most common infections worldwide[2]. Moreover, it possesses multiple virulence factors, and thus, it can develop strong resistance to antibacterial agents[3]. Bacterial culture has been considered an ideal tool for detecting S. aureus. The main disadvantages of this technique are time-consuming, excessive overloads on the operator, and high demands on the laboratory environment[4]. Quantitative polymerase chain reaction (PCR) has attracted great attentions as it can decrease the analysis time and amplify the bacterial genome exponentially. However, polymerase enzyme can be inhibited by matrix-related factors such as a low count of target bacteria in large sample volumes[5]. Thus, it is vital to construct selective, sensitive, and cost-effective sensors to detect *S. aureus*. Electroanalytical techniques have drawn great attentions as a result of fast response, sufficient selectivity, low detection limits, simplicity, and low cost[6–12].

Aptamer (Apt), a single-stranded DNA, has attracted much attentions as an alternative to antibodies due to its resistance to denaturation, ease of modification, and large scale chemical synthesis[13–15]. Upon binding to the target molecule, it can be folded into a unique 3D-conformation[16]. Molecular imprinted technology (MIT) was used to prevent the interference of very similar structures in different matrices. It was formed by the electro-polymerization of the functional monomer around the template. Specific binding sites are formed after the removal of the template, capable of identifying the analyte under study[17–20]. Interestingly, we found only one report in the literature describing the electrochemical sensing of *Pseudomonas aeruginosa* based on the fabrication of molecular imprinted aptasensor immobilized on gold nanoparticles/polydopamine hybrid[21].

Magnetic nanoparticles (Fe_3O_4 NPs) have been given a lot of interests due to its excellent electro-catalytic properties, low cost, low toxicity, and super paramagnetic properties[22,23]. In addition, noble metals e.g. AuNPs are used to modify electrodes to increase the conductivity and enhance the electron transfer[24,25].

[1]Department of Pharmaceutical Analytical Chemistry, Faculty of Pharmacy, Assiut University, Assiut 71524, Egypt. [2]Department of Microbiology and Immunology, Faculty of Pharmacy, Al-Azhar University, Assiut Branch, Assiut 71524, Egypt. [3]Department of Medical Biochemistry and Microbiology, Uppsala University, Uppsala, Sweden. [4]Department of Pharmaceutical Analytical Chemistry, Faculty of Pharmacy, Al-Azhar University, Assiut Branch, Assiut 71524, Egypt. ✉email: mohamed.elwakeel@pharm.aun.edu.eg

Herein, a molecular imprinted aptasensor was prepared for selective and sensitive detection of *S. aureus*. The aptasensor is based on the modification of magnetic nanoparticles with gold nanoparticles (AuNPs@Fe_3O_4). The molecular imprinted polymer film was formed around AuNPs@Fe_3O_4 in the presence of *S. aureus* and apt via electro-polymerization of o-phen monomer. After removing the *S. aureus*, an apt-MIP is made accessible for *S. aureus* influx. The as-fabricated aptasensor was applied efficiently to determine *S. aureus* in water, milk, and apple juice samples. To the best of our knowledge, this is the first report that use Apt-MIP for targeting *S. aureus*.

Experimental

Materials, reagents, and instruments. Details for descriptions of materials, reagents, and instruments were listed in Electronic Supplementary Materials (ESM).

Synthesis of magnetic nanoparticles (Fe_3O_4 NPs). According to our previous work[22], the magnetic nanoparticles were prepared with slight modifications. Briefly, 2.85 g $FeCl_3{\cdot}6H_2O$ and 1.24 g $FeCl_2{\cdot}4H_2O$ were sonicated in 35 mL DDW for 15 min until complete solubility. After that, 45 mL 1.5 M NaOH was added portion wise with continual stirring for another 15 min. The obtained black precipitate was washed with DDW and 15 mL $HClO_4$. Then, the precipitate was dried in an oven at 37 °C for 3 h before washing four times with DDW. Finally, the black product was dried at 60 °C overnight and then ground and stored at 4 °C.

Activation and preparation of aptamer (apt). The apt was firstly activated at 90 °C for 15 min. After that, 150 µL of 2.5 µM apt in TBST buffer. Then, it was incubated with 10^7 CFU mL^{-1} of *S. aureus* for 45 min at 37 °C.

Preparation of AuNPs@Fe_3O_4/GCE. The GCE was polished until a shiny appearance using alumina slurry, methanol, and DDW. A volume of 5 µL Fe_3O_4 (5.0 mg mL^{-1}) dispersed in ethanol was casted on the surface of GCE. After drying, gold nanoparticles (AuNPs) were electrodeposited on the surface of Fe_3O_4/GCE by immersion in 0.5 M Na_2SO_4 containing 1.5 mM $HAuCl_4$ solution under a constant potential of − 0.2 V for 300 s.

Fabrication of MIP-apt-AuNPs@Fe_3O_4/GCE. Firstly, 10.0 µL of the *S. aureus*-apt complex (prepared in "Activation and preparation of aptamer (apt)") was dropped on the surface of the AuNPs/Fe_3O_4/GCE where apt was covalently bound to AuNPs by strong Au–S bond. Then, Then, 15 µL of the *S. aureus* was cast on the electrode's surface to impregnate any free apt. Secondly, 1.45 mM o-phen was electro-polymerized on the surface of the electrode by sweeping the potential in the range of -0.4–0.9 V using a scan rate 100 mV s^{-1} for 15 cycles. Finally, the electrode was placed in a solution containing 0.01 M SDS and 7% HNO_3 (dissolved in DDW) for 60 min to remove *S. aureus* from its imprinted sites. A non-imprinted polymer (NIP) was prepared using the same steps without adding the template (*S. aureus*) (Fig. 1).

Preparation of real samples. The milk sample (0.5 mL) was mixed with 1.5 mL acetonitrile and spiked with *S. aureus* before shaking for 30 s. The mixture was sonicated for 5 min and then centrifuged at 3000 rpm for 10 min, and the supernatant was collected for further analysis. Drug-free milk samples were prepared using the same steps without spiking with *S. aureus*[26]. Conduit water was filtered to remove the insoluble and floated matters and stored in high-quality clean polyethylene containers. Water samples (5.0 mL) were spiked with different concentrations of *S. aureus* and stored at − 4 °C until analysis[22,27,28]. Apple juice samples obtained from the local market were analyzed without any further treatment.

Results and discussions

Characterization of nanocomposites. Scanning Electron Microscope (SEM) was used to check the different synthesized nanomaterials as depicted in Fig.S1. Magnetic nanoparticles (Fe_3O_4 NPs) are uniformly distributed with an average size of 14.5 nm (Fig. S1A). After modification with AuNPs, the size was increased to 38.5 nm, suggesting the successful decoration of Fe_3O_4 NPs with AuNPs (Fig. S1B). Functional monomer (o-phen) was electro-polymerized on the surface of AuNPs@Fe_3O_4/GCE in the presence of template (*S. aureus*) and thiolated apt, resulting in the complete coverage with a film of o-phen polymer (NIP) (Fig. S1C). After the removal of *S. aureus* from its imprinted sites, narrow pores were formed on the surface of polymer network resulting in the formation of molecular imprinted polymer (MIP) film (Fig. S1D). Fig.S2 shows the energy dispersive X-ray spectroscopy (EDX) of AuNPs@Fe_3O_4 nanocomposite with the main elements of O, Fe, and Au. Fig.S3 exhibits the FTIR spectra of Fe_3O_4 (green), AuNPs@Fe_3O_4 (red), and apt-AuNPs@Fe_3O_4 (black) where absorption bands at 3420, 1705, 1470, and 615 cm^{-1} are ascribed to υ (OH) of surface adsorbed water, υ (C=O), δ (OH), and υ (Fe–O), respectively[22]. In addition, Fig. S4 shows the Zeta potentials of the as-synthesized nanocomposites including Fe_3O_4, AuNPs/Fe_3O_4, and apt- AuNPs/Fe_3O_4. The obtained Zeta potential values of Fe_3O_4, AuNPs/Fe_3O_4, and apt- AuNPs/Fe_3O_4 were found to be 32.8 ± 0.56, 22.3 ± 1.09, and 10.23 ± 1.57, respectively. It is seen that the potential values decrease after coupling of positively charged Fe_3O_4 with AuNPs followed by further decrease upon binding with negatively charged apt, suggesting the successful formation of apt- AuNPs/Fe_3O_4.

Electrochemical characterization of the as-synthesized nanocomposites. Different electrodes were prepared and evaluated using cyclic voltammetry (CV) and electrochemical impedance spectroscopy (EIS). They were immersed in a solution of 5.0 mM $Fe(CN)_6^{3-/4-}$ dissolved in 0.1 M KCl. Figure 2A_a exhibits the redox peaks of $Fe(CN)_6^{3-/4-}$ at bare GCE where it shows to identifiable and separated anodic and cathodic peaks. After modification with Fe_3O_4 NPs, the redox currents of the redox probe were increased as a result of enhanced

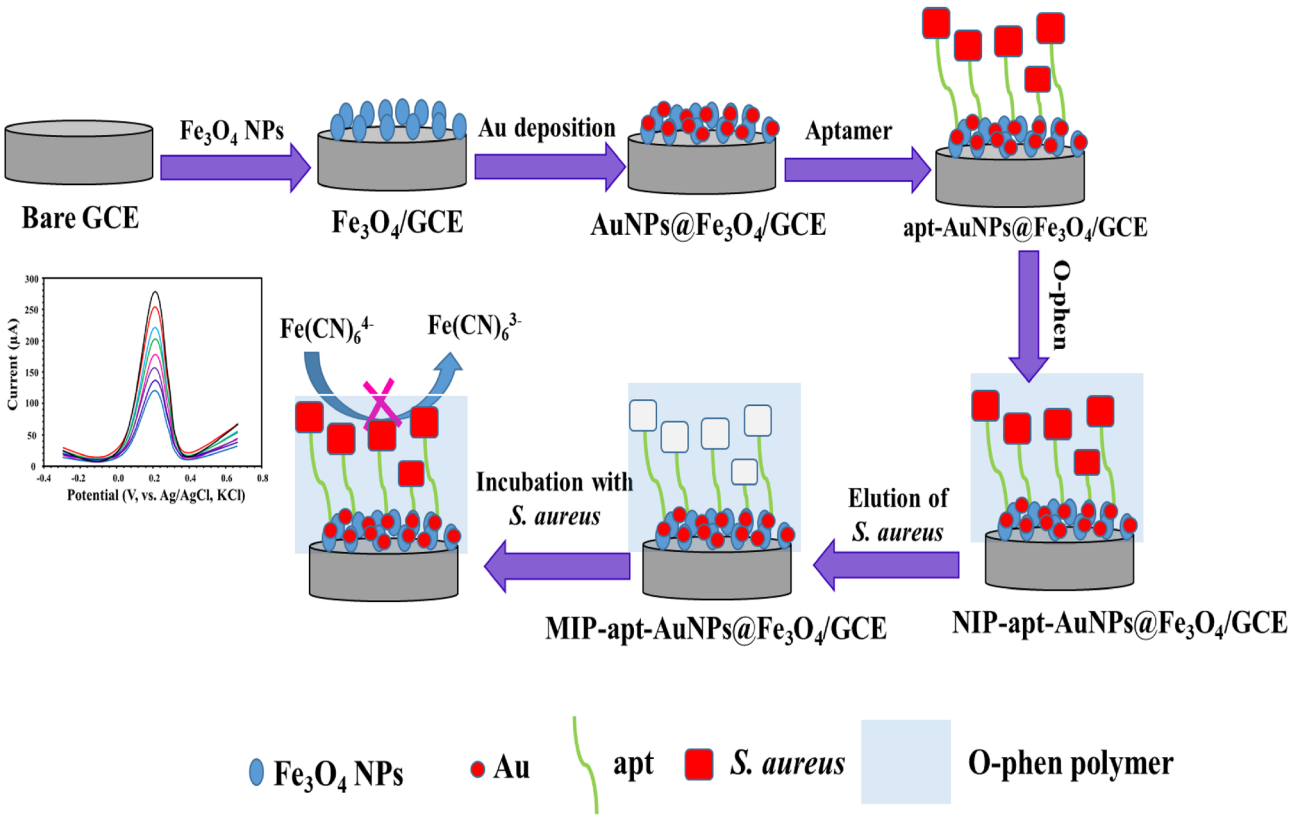

Figure 1. Representative diagram for the fabrication of the molecularly imprinted based aptasensor and its use for the determination of *S. aureus*.

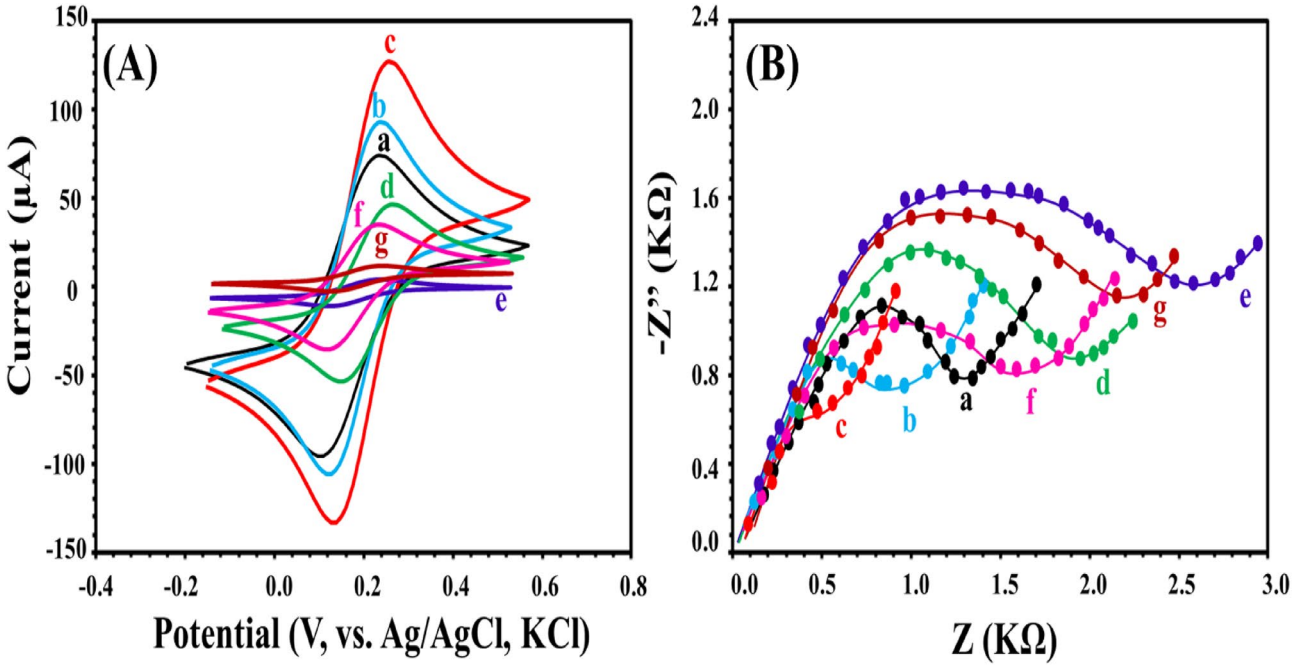

Figure 2. CV (**A**) and EIS (**B**) of bare GCE (a), Fe_3O_4/GCE (b), AuNPs@ Fe_3O_4/GCE (c), apt-AuNPs@ Fe_3O_4/GCE (d), NIP-apt-AuNPs@ Fe_3O_4/GCE (e), MIP-apt-AuNPs@ Fe_3O_4/GCE (f), and MIP-apt-AuNPs@ Fe_3O_4/GCE after rebinding of *S. aureus* (g). Conditions are 5.0 mM $Fe(CN)_6^{3-/4-}$ dissolved in 0.1 M KCl.

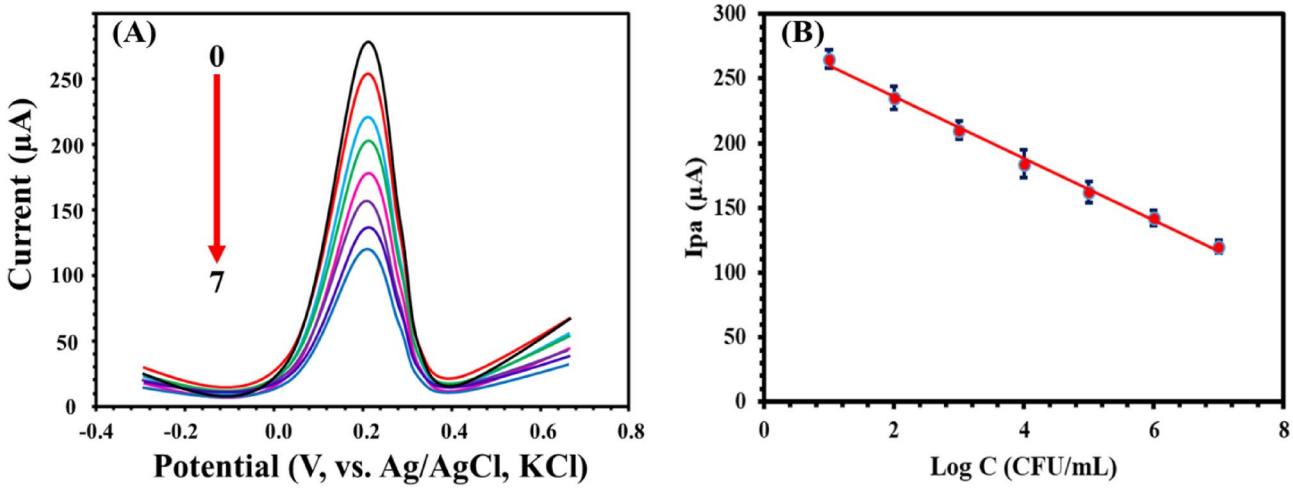

Figure 3. (**A**) DPVs of MIP-apt-AuNPs@ Fe_3O_4/GCE after incubation with different concentrations of the *S. aureus* (0:0, $1{:}10^1$, $2{:}10^2$, $3{:}10^3$, 4: 10^4, $5{:}10^5$, 6: 10^6 and 7: 10^7 CFU·mL^{-1} *S. aureus* in 0.1 M KCl containing 5.0 mM $[Fe(CN)_6]^{3-/4-}$ and (**B**) is a calibration plot. Conditions of DPV are pulse height of 30 mV, pulse width of 0.08 s and step height of 15 mV.

surface area and good conductivity of Fe_3O_4 NPs (Fig. 2Ab). Further enhancement of the redox currents was observed after modification with AuNPs (Fig. 2Ac), suggesting the excellent conductivity of AuNPs. Attachment of apt to the surface of AuNPs@ Fe_3O_4/GCE resulted in the decrease of the peak currents of $Fe(CN)_6^{3-/4-}$ due to the repulsion between the negatively charged apt and negatively charged redox probe (Fig. 2Ad). Electropolymerization of o-phen monomer on the surface of apt- AuNPs@ Fe_3O_4/GCE and in the presence of *S. aureus* i.e. NIP- apt- AuNPs@ Fe_3O_4/GCE, the peak currents of $Fe(CN)_6^{3-/4-}$ were sharply deceased due to the formation of insulating layer that inhibited the influx of the redox probe (Fig. 2Ae). The removal of *S. aureus* from its imprinted sites i.e. MIP- apt- AuNPs@ Fe_3O_4/GCE increased the peak currents of $Fe(CN)_6^{3-/4-}$ due to the creation of numerous imprinted sites for the flowing of the redox probe, but it is still lower than apt- AuNPs@ Fe_3O_4/GCE (Fig. 2Af). After rebinding the *S. aureus*, the peak currents of the redox probe were dramatically decreased as the cavities of the imprinted layers were relocked by the template (Fig. 2Ag). Moreover, the electrochemical activities of different interfaces were demonstrated using EIS (Fig. 2B). It is shown that the semicircle diameter was changed after each modification.

Optimization of experimental conditions. Optimizations of incubation time, pH effect, elution time, deposition potential and time of AuNPs, and apt concentration were listed in ESM.

Analytical figures of merit. The sensitivity of the proposed aptasensor towards *S. aureus* was measured using differential pulse voltammetry (DPV) under optimized conditions. Figure 3A shows that the peak currents of the redox probe at MIP-apt-AuNPs@ Fe_3O_4/GCE were decreased after the increase in the concentration of *S. aureus*. The calibration plot shown in Fig. 3B was linear over the range of 10^1–10^7 CFU mL^{-1} with a linear regression of Ipa (µA) = − 23.9 Log $C_{S.\ aureus}$ + 283.9 (R^2 = 0.9986). According to IUPAC recommendation (IUPAC 1976), the analyte's signal at the detection limit (S_{dl}) is given by:

$$S_{dl} = S_{reag} + k * \sigma_{reag,}$$

where S_{reag} is the electrochemical signal for a blank, σreag is the known standard deviation for the blank's electrochemical signal (n = 10). As is well known, k = signal/noise (S/N) = 3. As suggested by Long and Winefordner (1983) (Long and Winefordner 1983), the use of k = 3 allows a confidence level of 99.86% for a normal distribution of the blank signals. The detection limit can be calculated by S_{dl} and calibration curves. The LOD was calculated as 1 CFU mL^{-1}. Moreover, the method with compared with other reported methods for the determination of S. aureus (Table 1). I t was found that the proposed aptasensor exhibits wide-linear range and low detection value.

Reproducibility, repeatability, and stability of MIP-apt-AuNPs@ Fe_3O_4/GCE. Reproducibility was measured by monitoring the DPV responses of five fabricated aptasensor prepared under the same conditions (Fig. 4A). It was found that the relative standard deviation % (RSD %) did not exceed 3.2%. Moreover, the repeatability was measured via measuring the DPV responses for six readings and calculating the RSD % that did not exceed 2.6% (Fig. 4B).

Moreover, the stability of the aptasensor was examined using CV at scan rate of 300 mV s^{-1} in 0.1 M phosphate buffer and 5.0 mM $[Fe(CN)_6]^{3-/4-}$. After 50 cycles, DPV readings did not appreciably change, confirming the excellent stability of the proposed sensor (Fig. S10A). In addition, the long term stability of the aptasensor was studied by storing the aptasensor at 4 °C and it was used to detect *S. aureus* every week for one month (Fig.S10 B). It was found that the proposed aptasensor retained about 95% of its original activity for four weeks.

Sensor	Method	Linear range (CFU mL^{-1})	LOD (CFU mL^{-1})	Reference
Apt/single walled carbon nanotubes	Potentiometry	10^3–10^8	8×10^2	[29]
Apt/reduced graphene oxide/AuNPs	Impedimetry	10^1–10^6	10	[30]
Apt/Au electrode	Impedimetry	10^1–10^4	10	[31]
Apt/S. aureus/apt-AgNP sandwich complex	DPV	10^1–10^6	1	[32]
Apt/AuNPs/carbon nanoparticles/cellulose nanofibers	Impedimetry	1.2×10^1–1.2×10^8	1	[33]
MIP-apt-AuNPs@ Fe_3O_4/GCE	**DPV**	**10^1–10^7**	**1**	**This work**

Table 1. Comparison between the proposed aptasensor and other reported sensors for the determination of *S. aureus*.

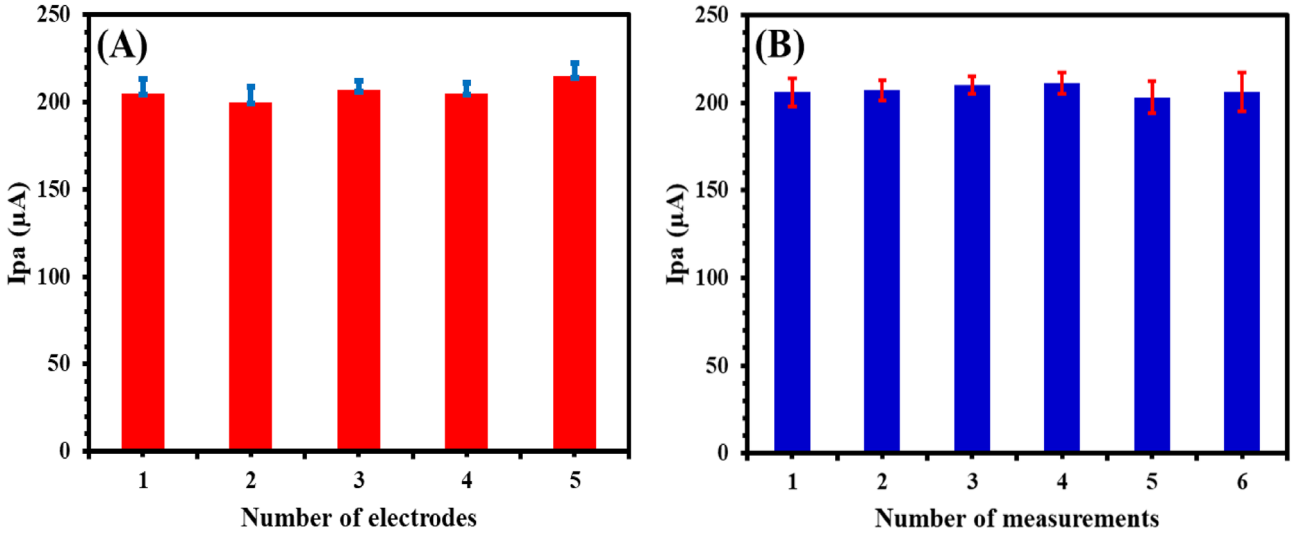

Figure 4. Reproducibility (**A**) and repeatability (**B**) of MIP-apt-AuNPs@ Fe_3O_4/GCE after incubation with of the 10^3 CFU mL^{-1} *S. aureus* in 0.1 M KCl containing 5.0 mM $[Fe(CN)_6]^{3-/4-}$. Conditions of DPV are pulse height of 30 mV, pulse width of 0.08 s and step height of 15 mV.

Specificity of MIP-apt-AuNPs@ Fe_3O_4/GCE. The specificity of the as-fabricated aptasensor was evaluated by immersing in 10^3 CFU contained in 300 µM organic compounds such as urea, glucose, ascorbic acid, uric acid, methionine, glycine, alanine, lysine, arginine, and lactic acid. Moreover, CV responses of the as-prepared aptasensor were recorded in the presence of 10^6 CFU mL^{-1} *Klebsiella pneumonia (K. pneumonia)*, *Escherichia coli* (*E. coli*,), *Pseudomonas aeruginosa (P. aeruginosa)*, *Listeria monocytogenes* (*L. monocytogenes*), and *Candida albicans (C. albicans)*. Figures 5 A&B show that slight variations in currents were observed after addition of interfering compounds and bacteria. Moreover, it is obvious that only *S. aureus* can decrease the currents of redox probe, which is attributed to the molecular imprinted spaces and apt are well fitted for *S. aureus*.

Applications of MIP-apt-AuNPs@ Fe_3O_4/GCE. We tested the aptasensor for the detection of S. aureus in milk, conduit water, and apple juice samples. The concentration of *S. aureus* was adjusted to 0.5 McFarland turbidity. After that, the samples were spiked with different concentrations of *S. aureus*. Table 2 shows that the recoveries % ranged from 96 to 104% with relative standard deviations (RSDs) less than 3.4%, suggesting the suitability of the aptasensor for measuring *S. aureus* in milk, conduit water, and apple juice samples. Calibration plots for different artificial samples were shown in Fig. 6.

Conclusion

In this context, an ultrasensitive and selective molecular imprinted based aptasensor was fabricated to detect S. aureus. The aptasensor consists of gold nanoparticles modified magnetic nanoparticles loaded on the glassy carbon electrode surface (AuNPs@ Fe_3O_4/GCE). The thiolated aptamer was attached to the nanocomposite surface via Au–S covalent bond. A polymer film was deposited over the surface of the AuNPs@ Fe_3O_4/GCE by electro-polymerization of o-phen in the presence of the template (*S. aureus*). After elution of the template, the formed imprinted cavities were formed that can extract *S. aureus* from the complicated matrices. Simplicity, low LOD, good stability, low cost, high sensitivity, and high selectivity are the main advantages of the proposed aptasensor. The molecular imprinted aptasensor was applied efficiently for the detection of *S. aureus* in milk, conduit water, and apple juice samples.

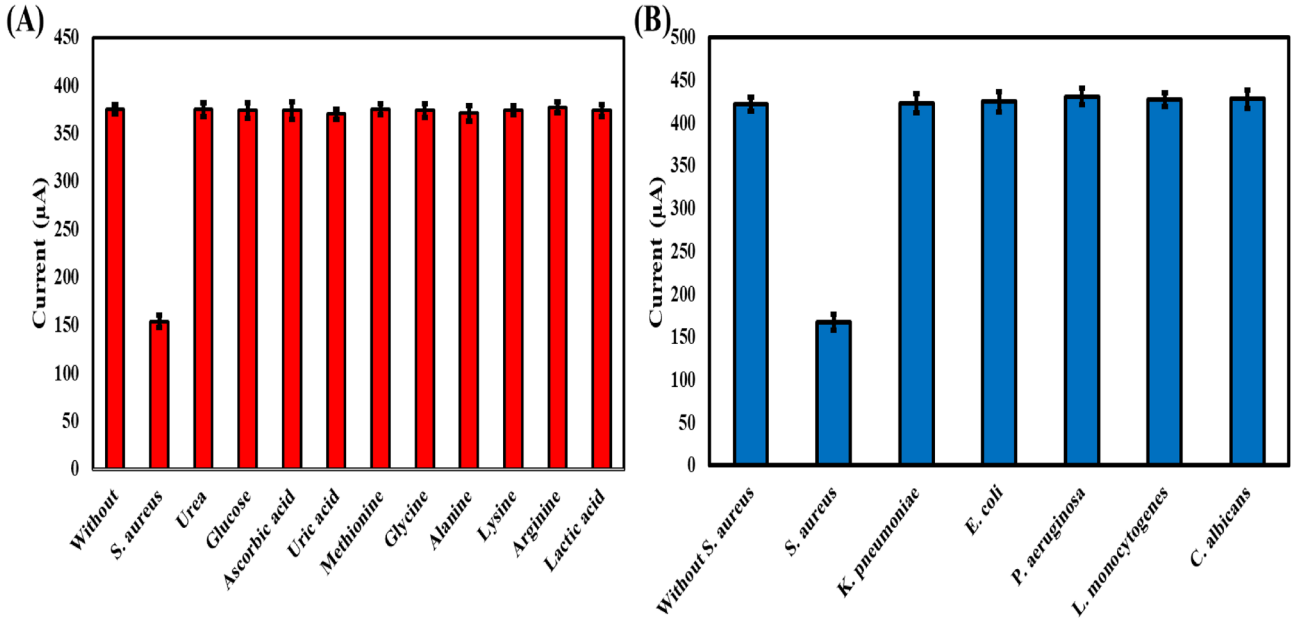

Figure 5. (**A**) CV scans of MIP-apt-AuNPs@ Fe_3O_4/GCE in presence of 10^3 CFU mL^{-1} *S. aureus* and 300 μM some common organic compounds in 0.1 M phosphate buffer containing 5.0 mM $[Fe(CN)_6]^{3-/4-}$ at $\nu = 300$ mV s^{-1}. (B) CV scans of MIP-apt-AuNPs@ Fe_3O_4/GCE in presence of 10^3 CFU mL^{-1} *S. aureus* and 10^6 CFU mL^{-1} interfering bacteria in 0.1 M phosphate buffer containing 5.0 mM $[Fe(CN)_6]^{3-/4-}$ at $\nu = 300$ mV s^{-1}.

Sample	Added (CFU mL^{-1})	Found (CFU mL^{-1})	Recovery % ± SD	RSD %
Milk				
1	10^2 10^4	1.02×10^2 1.02×10^4	102 ± 2.9 102 ± 3.4	2.8 3.3
2	10^2 10^4	1.03×10^2 0.99×10^4	103 ± 2.3 99 ± 2.7	2.2 2.7
3	10^2 10^4	1.00×10^2 1.02×10^4	100 ± 2.7 102 ± 3.4	2.7 3.3
Conduit water				
1	10^2 10^4	1.01×10^2 0.98×10^4	101 ± 2.3 98 ± 2.9	2.2 3.0
2	10^2 10^4	0.99×10^2 0.96×10^4	99 ± 3.0 96 ± 2.0	3.0 3.4
3	10^2 10^4	1.03×10^2 1.04×10^4	103 ± 3.5 104 ± 2.7	3.4 2.6
Apple juice				
1	10^2 10^4	0.99×10^2 0.98×10^4	99 ± 2.8 98 ± 3.0	2.8 3.1
2	10^2 10^4	1.01×10^2 1.00×10^4	101 ± 3.1 100 ± 2.7	3.1 2.7
3	10^2 10^4	0.97×10^2 0.99×10^4	97 ± 2.5 99 ± 2.8	2.6 2.8

Table 2. Applications of MIP-apt-AuNPs@ Fe_3O_4/GCE for the determination of S. aureus in milk, conduit water, and apple juice samples.

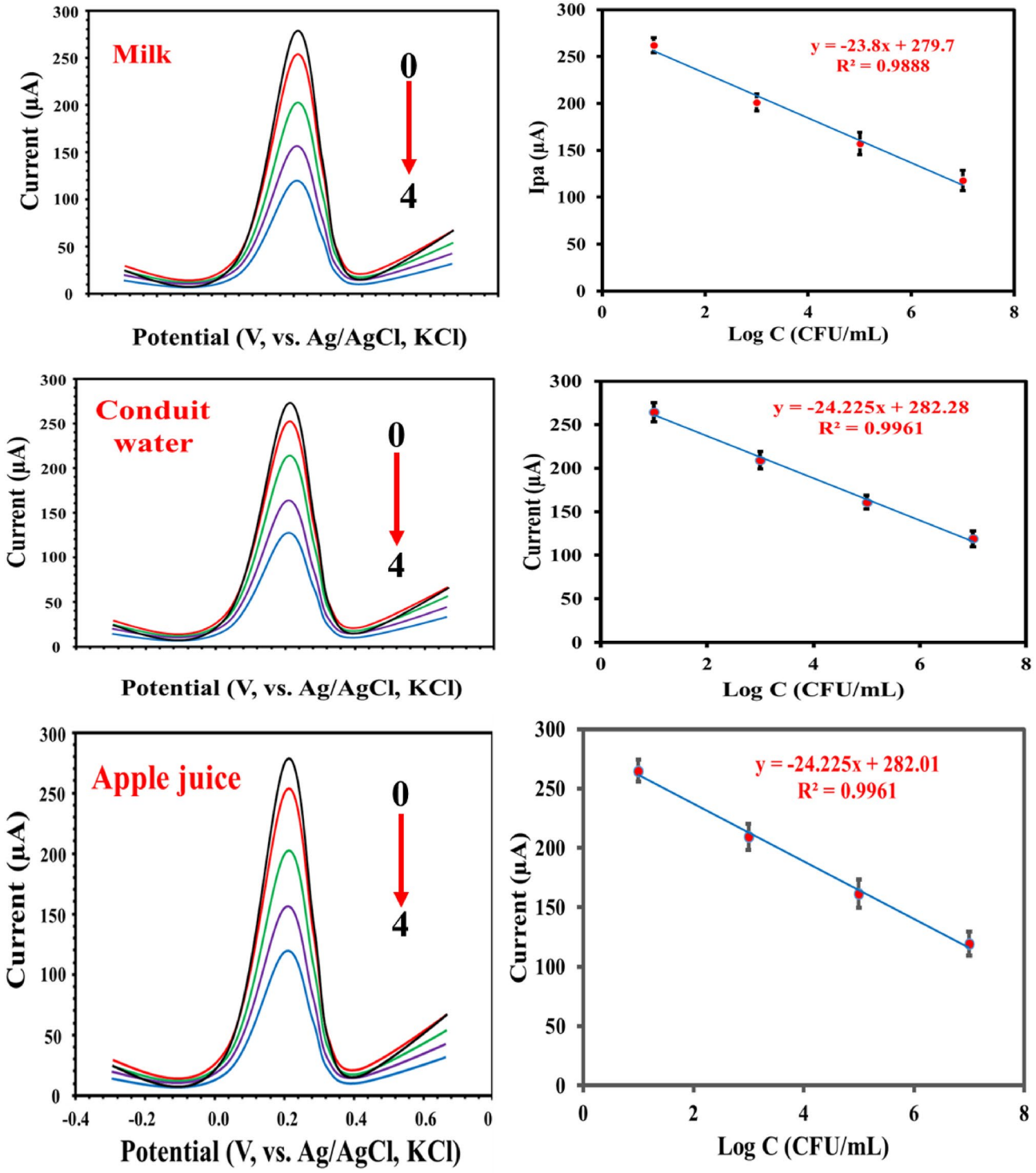

Figure 6. DPVs of MIP-apt-AuNPs@ Fe_3O_4/GCE after incubation with different concentrations of the *S. aureus* (0:0, $1:10^1$, $2:10^3$, $4:10^5$, and $4: 10^7$ CFU·mL^{-1} *S. aureus* in milk, conduit water, and apple juice samples. Conditions are concentration of $[Fe(CN)_6]^{3-/4-}$ = 5.0 mM, pulse height of 30 mV, pulse width of 0.08 s, and step height of 15 mV.

Data availability

All data generated or analyzed during this study are included in this published article and its supplementary information files.

Received: 15 April 2022; Accepted: 27 June 2022
Published online: 22 July 2022

References

1. Tong, S. Y., Davis, J. S., Eichenberger, E., Holland, T. L. & Fowler, V. G. Staphylococcus aureus infections: Epidemiology, pathophysiology, clinical manifestations, and management. *Clin. Microbiol. Rev.* **28**, 603–661 (2015).
2. Chang, Y. C. *et al.* Rapid single cell detection of *Staphylococcus aureus* by aptamer-conjugated gold nanoparticles. *Sci. Rep.* **3**, 1863 (2013).
3. Cai, R., Yin, F., Zhang, Z., Tian, Y. & Zhou, N. Functional chimera aptamer and molecular beacon based fluorescent detection of *Staphylococcus aureus* with strand displacement-target recycling amplification. *Anal. Chim. Acta* **1075**, 128–136 (2019).
4. Reta, N., Saint, C. P., Michelmore, A., Simon, B. P. & Voelcker, N. H. Nanostructured electrochemical biosensors for label-free detection of water-and food-borne pathogens. *ACS Appl. Mater. Interfaces* **10**, 6055–6072 (2018).
5. Wang, Y. & Salazar, J. K. Culture-independent rapid detection methods for bacterial pathogens and toxins in food matrices. *Compr. Rev. Food Sci. F.* **15**, 183–205 (2016).
6. Mohamed, F. A., Khashaba, P. Y., Shahin, R. Y. & El-Wekil, M. M. A determination approach for rivastigmine by lepidocrocite nanoparticles supported on N-chitosan carbon nanosheets/anti-Fouling PAS: Application to biosensing. *J. Electrochem. Soc.* **166**, H41–H46 (2019).
7. Mahnashi, M. H., Mahmoud, A. M., Alkahtani, S. A., Ali, R. & El-Wekil, M. M. Facile fabrication of a novel disposable pencil graphite electrode for simultaneous determination of promising immunosuppressant drugs mycophenolate mofetil and tacrolimus in human biological fluids. *Anal. Bioanal. Chem.* **412**, 355–364 (2020).
8. El-Wekil, M. M., Abdelhady, K. K., Abdel Salam, R. A., Hadad, H. G. & Ali, R. Facile synthesis of novel nanocomposite prepared from spinel copper ferrite and reduced graphene oxide in the presence of anti-fouling agent diethyl ammonium acid sulphate for ultrasensitive detection of rosuvastatin in human plasma. *Microchem. J.* **147**, 1133–1140 (2019).
9. Alkahtani, S. A., El-Wekil, M. M., Mahmoud, A. M., Mahnashi, M. H. & Oraby M,. One pot synthesis of AuPdPt trimetallic nanohybrid decorated reduced graphene oxide nanosheets for ultrasensing of anti-convulsant drug retigabine (Ezogabine). *J. Electrochem. Soc.* **166**, 521–526 (2019).
10. El-Wekil, M. M., Mahmoud, A. M., Alkahtani, S. A., Marzouk, A. A. & R. Ali R.,. A facile synthesis of 3D $NiFe_2O_4$ nanospheres anchored on a novel ionic liquid modified reduced graphene oxide for electrochemical sensing of ledipasvir: Application to human pharmacokinetic study. *Biosens. Bioelectron.* **109**, 164–170 (2018).
11. Alkahtani, S. A., Mahmoud, A. M., Mahnashi, M. H., Ali, R. & El-Wekil, M. M. Facile fabrication of a novel 3D rose like lanthanum doped zirconia decorated reduced graphene oxide nanosheets: An efficient electro-catalyst for electrochemical reduction of futuristic anti-cancer drug salinomycin during pharmacokinetic study. *Biosens. Bioelectron.* **150**, 111849 (2020).
12. Mahnashi, H. M., Mahmoud, A. M., Alkahtani, A. S. & El-Wekil, M. M. Simultaneous electrochemical detection of azithromycin and hydroxychloroquine based on VS_2 QDs embedded N, S @graphene aerogel/cCNTs 3D nanostructure. *Microchem. J.* **163**, 105925 (2021).
13. Röthlisberger, P. & Hollenstein, M. Aptamer chemistry. *Adv. Drug Deliv. Rev.* **134**, 3–21 (2018).
14. Mahmoud, A. M., Alkahtani, S. A., Alyami, B. A. & El-Wekil, M. M. Dual-recognition molecularly imprinted aptasensor based on gold nanoparticles decorated carboxylated carbon nanotubes for highly selective and sensitive determination of histamine in different matrices. *Anal. Chim. Acta* **1133**, 58–65 (2020).
15. El-Wekil, M. M., Darweesh, M., Shaykoon, MSh. A. & Ali, R. Enzyme-free and label-free strategy for electrochemical oxaliplatin aptasensing by using rGO/MWCNTs loaded with AuPd nanoparticles as signal probes and electro-catalytic enhancers. *Talanta* **217**, 121084 (2020).
16. Sun, H. & Zu, Y. A highlight of recent advances in aptamer technology and its application. *Molecules* **20**, 11959–11980 (2015).
17. Mahnashi, M. H. *et al.* Enhanced molecular imprinted electrochemical sensing of histamine based on signal reporting nanohybrid. *Microchem. J.* **168**, 106439 (2021).
18. El-Wekil, M. M., Mahmoud, A. M., Marzouk, A. A., Alkahtani, S. A. & Ali, R. A novel molecularly imprinted sensing platform based on MWCNTs/AuNPs decorated 3D starfish like hollow nickel skeleton as a highly conductive nanocomposite for selective and ultrasensitive analysis of a novel pan-genotypic inhibitor velpatasvir in body fluids. *J. Mol. Liq.* **271**, 105–111 (2018).
19. Mahmoud, A. M., El-Wekil, M. M., Mahnashi, M. H., Ali, M. F. B. & Alkahtani, S. A. Modification of N, S co-doped graphene quantum dots with p-aminothiophenol-functionalized gold nanoparticles for molecular imprint-based voltammetric determination of the antiviral drug sofosbuvir. *Microchim. Acta* **186**, 617 (2019).
20. Mahnashi, M. H. *et al.* Ultrasensitive and selective molecularly imprinted electrochemical oxaliplatin sensor based on a novel nitrogen-doped carbon nanotubes/Ag@cu MOF as a signal enhancer and reporter nanohybrid. *Microchim. Acta* **188**, 124 (2021).
21. Sarabaegi, M. & Roushani, M. Rapid and sensitive determination of Pseudomonas aeruginosa by using a glassy carbon electrode modified with gold nanoparticles and aptamer-imprinted polydopamine. *Microchem. J.* **168**, 106388 (2021).
22. El-Wekil, M. M., Ali, H. R. H., Marzouk, A. A. & Ali, R. Synthesis of Fe_3O_4 nanobead-functionalized 8-hydroxyquinoline sulfonic acid supported by an ion-imprinted biopolymer as a recognition site for Al^{3+} ions: estimation in human serum and water samples. *New J. Chem.* **42**, 9828–9836 (2018).
23. Ali, H. R. H., Hassan, A. I., Hassan, Y. F. & El-Wekil, M. M. Mannitol capped magnetic dispersive micro-solid-phase extraction of polar drugs sparfloxacin and orbifloxacin from milk and water samples followed by selective fluorescence sensing using boron-doped carbon quantum dots. *J. Environ. Chem. Engin.* **9**, 105078 (2021).
24. Wei, J. *et al.* Adsorbent assisted in situ electrocatalysis: An ultra-sensitive detection of As (III) in water at Fe_3O_4 nanosphere densely decorated with Au nanoparticles. *Anal. Chem.* **88**, 1154–1161 (2016).
25. Li, S. S. *et al.* Surface Fe (II)/Fe (III) cycle promoted ultra-highly sensitive electrochemical sensing of arsenic (III) with dumbbell-like Au/Fe_3O_4 nanoparticles. *Anal. Chem.* **90**, 4569–4577 (2018).
26. Ali, H. R. H., Hassan, A. I., Hassan, Y. F. & El-Wekil, M. M. Mannitol capped magnetic dispersive micro-solid-phase extraction of polar drugs sparfloxacin and orbifloxacin from milk and water samples followed by selective fluorescence sensing using boron-doped carbon quantum dots. *J. Environ. Chem. Eng.* **9**, 105078 (2021).
27. Mahnashi, M. H., Mahmoud, A. M., Alkahtani, S. A., Ali, R. & El-Wekil, M. M. A novel imidazole derived colorimetric and fluorometric chemosensor for bifunctional detection of copper (II) and sulphide ions in environmental water samples. *Spectrochim. Acta Part A Mol. Biomol. Spectrosc.* **228**, 117846 (2020).
28. Alyami, B. A., Mahmoud, A. M., Alkahtani, S. A. & El-Wekil, M. M. $NiFe_2O_4$ nanospheres functionalized with 2-(2, 4-Dihydroxyphenyl)-3, 5, 7-trihydroxychromen-4-one for selective solid-phase microextraction of aluminium. *Talanta* **226**, 122167 (2021).
29. Zelada-Guillén, G. A., Sebastián-Avila, J. L., Blondeau, P., Riu, J. & Rius, F. X. Label-free detection of *Staphylococcus aureus* in skin using real-time potentiometric biosensors based on carbon nanotubes and aptamers. *Biosens. Bioelectron.* **31**, 226–232 (2012).
30. Jia, F. *et al.* Impedimetric aptasensor for *Staphylococcus aureus* based on nanocomposite prepared from reduced graphene oxide and gold nanoparticles. *Microchim. Acta* **181**, 967–974 (2014).
31. Reich, P., Stoltenburg, R., Strehlitz, B., Frense, D. & Beckmann, D. Development of an impedimetric aptasensor for the detection of *Staphylococcus aureus*. *Int. J. Mol. Sci.* **18**, 2484–2501 (2017).
32. Abbaspour, A., Norouz-Sarvestani, F., Noori, A. & Soltani, N. Aptamer-conjugated silver nanoparticles for electrochemical dual-aptamer-based sandwich detection of *Staphylococcus aureus*. *Biosens. Bioelectron.* **68**, 149–155 (2015).

33. Ranjbar, S. & Shahrokhian, S. Design and fabrication of an electrochemical aptasensor using Au nanoparticles/carbon nanoparticles/cellulose nanofibers nanocomposite for rapid and sensitive detection of *Staphylococcus aureus*. *Bioelectrochemistry* **123**, 70–76 (2018).

Author contributions

M.M.E. carried out the electrochemical analysis, wrote, and design the manuscript with added references and background text. H.M.H., M.D., M.E.A., R.A. wrote part of the literature review and aid in the preparation of bacterial strains and materials used for the electrochemical determination.

Funding

Open access funding provided by The Science, Technology & Innovation Funding Authority (STDF) in cooperation with The Egyptian Knowledge Bank (EKB).

Competing interests

The authors declare no competing interests.

Additional information

Supplementary Information The online version contains supplementary material available at https://doi.org/10.1038/s41598-022-15637-1.

Correspondence and requests for materials should be addressed to M.M.E.-W.

Reprints and permissions information is available at www.nature.com/reprints.

Publisher's note Springer Nature remains neutral with regard to jurisdictional claims in published maps and institutional affiliations.